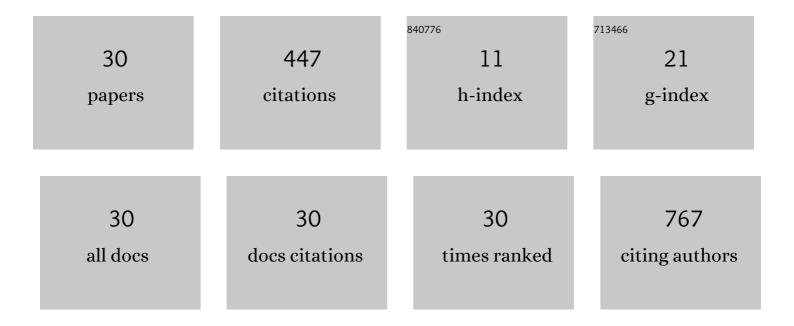
Matthias M L Arras

List of Publications by Year in descending order

Source: https://exaly.com/author-pdf/4652818/publications.pdf Version: 2024-02-01



#	Article	IF	CITATIONS
1	Electrospinning of aligned fibers with adjustable orientation using auxiliary electrodes. Science and Technology of Advanced Materials, 2012, 13, 035008.	6.1	92
2	<i>In Situ</i> Formation of Nanohybrid Shish-Kebabs during Electrospinning for the Creation of Hierarchical Shish-Kebab Structures. Macromolecules, 2016, 49, 3550-3558.	4.8	43
3	Electrodynamic control of the nanofiber alignment during electrospinning. Applied Physics Letters, 2013, 102, .	3.3	42
4	Biomimetic 3D hydroxyapatite architectures with interconnected pores based on electrospun biaxially orientated PCL nanofibers. RSC Advances, 2014, 4, 14833-14839.	3.6	41
5	The Interfacial Assembly of Polyoxometalate Nanoparticle Surfactants. Nano Letters, 2018, 18, 2525-2529.	9.1	37
6	Bulk and Surface Morphologies of ABC Miktoarm Star Terpolymers Composed of PDMS, PI, and PMMA Arms. Macromolecules, 2018, 51, 1041-1051.	4.8	18
7	Responsive copolymer–graphene oxide hybrid microspheres with enhanced drug release properties. RSC Advances, 2017, 7, 3720-3726.	3.6	17
8	Extended-Chain Induced Bulk Morphologies Occur at Surfaces of Thin Co-Oligomer Films. Macromolecules, 2012, 45, 4740-4748.	4.8	15
9	Alignment of multi-wall carbon nanotubes by disentanglement in ultra-thin melt-drawn polymer films. Carbon, 2013, 60, 366-378.	10.3	15
10	Studies on the 3-Lamellar Morphology of Miktoarm Terpolymers. Macromolecules, 2018, 51, 7491-7499.	4.8	14
11	pH-Dependent Ordered Fibrinogen Adsorption on Polyethylene Single Crystals. Langmuir, 2016, 32, 11868-11877.	3.5	13
12	High molar mass amphiphilic block copolymer enables alignment and dispersion of unfunctionalized carbon nanotubes in melt-drawn thin-films. Polymer, 2017, 127, 15-27.	3.8	11
13	Enveloping Self-Assembly of Carbon Nanotubes at Copolymer Micelle Cores. Langmuir, 2014, 30, 14263-14269.	3.5	10
14	How the Calorimetric Properties of a Crystalline Copolymer Correlate to Its Surface Nanostructures. Macromolecules, 2014, 47, 1705-1714.	4.8	9
15	Isotope Effects on the Crystallization Kinetics of Selectively Deuterated Poly(ε aprolactone). Journal of Polymer Science, Part B: Polymer Physics, 2019, 57, 771-779.	2.1	9
16	Mechanisms and kinetics of the crystal thickening of poly(butadiene)-block-poly(ethylene oxide) during annealing within the melting range. European Polymer Journal, 2015, 68, 10-20.	5.4	8
17	Nanocrystal Width Controls Fibrinogen Orientation and Assembly Kinetics on Poly(butene-1) Surfaces. Langmuir, 2017, 33, 6563-6571.	3.5	8
18	Lipid shape determination of detergent solubilization in mixed-lipid liposomes. Colloids and Surfaces B: Biointerfaces, 2020, 187, 110609.	5.0	8

MATTHIAS M L ARRAS

#	Article	IF	CITATIONS
19	Nanoconfinement and Sansetsukon-like Nanocrawling Govern Fibrinogen Dynamics and Self-Assembly on Nanostructured Polymeric Surfaces. Langmuir, 2018, 34, 14309-14316.	3.5	7
20	On the morphological behavior of ABC miktoarm stars containing poly(cis 1,4â€isoprene), poly(styrene), and poly(2â€vinylpyridine). Journal of Polymer Science, Part B: Polymer Physics, 2018, 56, 1491-1504.	2.1	6
21	Alternating crystalline lamellar structures from thermodynamically miscible poly(Îμ-caprolactone) H/D blends. Polymer, 2019, 175, 320-328.	3.8	5
22	3D model of intra-yarn fiber volume fraction gradients of woven fabrics. Composite Structures, 2017, 180, 944-954.	5.8	4
23	Chain arrangements of selectively deuterated poly(ε-caprolactone) copolymers as revealed by neutron scattering. Polymer, 2020, 193, 122375.	3.8	4
24	Modeling the saturation of detergent association in mixed liposome systems. Colloids and Surfaces B: Biointerfaces, 2021, 206, 111927.	5.0	3
25	Indirect morphological analysis of particles in polymer particle composites via non-destructive permittivity measurements. Composites Science and Technology, 2019, 169, 176-185.	7.8	2
26	Polystyrene Homopolymer Enhances Dispersion of MWCNTs Stabilized in Solution by a PS-b-P2VP Copolymer. Langmuir, 2021, 37, 391-399.	3.5	2
27	Classifying condition of ultra-high-molecular-weight polyethylene ropes with wide-angle X-ray scattering. Polymer Testing, 2022, 109, 107524.	4.8	2
28	An advanced geometrical model for laminated woven fabrics using Lamé exponents with enhanced accuracy. Journal of Composite Materials, 2018, 52, 1443-1455.	2.4	1
29	Acetabular Cup with a Trabecular Coating: A Novel Approach to a Monolithic Cup Made of One Highâ€Strength Ceramic Material. Advanced Engineering Materials, 2018, 20, 1800230.	3.5	1

30 Optofluidic Chip System with Integrated Fluidically Controllable Optics. , 2009, , .

0